ISSN 1062-8738, Bulletin of the Russian Academy of Sciences: Physics, 2023, Vol. 87, No. 6, pp. 715–719. © The Author(s), 2023. This article is an open access publication, corrected publication 2023.
Russian Text © The Author(s), 2023, published in Izvestiya Rossiiskoi Akademii Nauk, Seriya Fizicheskaya, 2023, Vol. 87, No. 6, pp. 813–818.

A Magnetic Field-Controlled Elastomer Composite Based on Porous Polydimethylsiloxane

A. A. Amirov[a, *], A. S. Kaminskiy[b], E. A. Arkhipova[c, d], N. A. Cherkasova[e], A. O. Tovpinets[a], V. N. Leucine[a], A. P. Pyatakov[b], V. E. Zhivulin[e], and V. V. Rodionova[a]

[a] *Immanuel Kant Baltic Federal University, Kaliningrad, 236041 Russia*
[b] *Department of Physics, Moscow State University, Moscow, 119991 Russia*
[c] *Peter the Great St. Petersburg Polytechnic University, St. Petersburg, 195251 Russia*
[d] *Ioffe Institute, St. Petersburg, 194021 Russia*
[e] *South Ural State University, Chelyabinsk, 454080 Russia*
**e-mail: amiroff_a@mail.ru*

Received December 5, 2022; revised December 23, 2022; accepted February 27, 2023

Abstract—Magnetic elastomers are obtained using polydimethylsiloxane polymer filled with barium hexaferrite microparticles that have a homogeneous and porous microstructure. The microstructure and magnetic and mechanical properties of the synthesized samples are studied. The way of leaching the filler yields magnetic elastomers with a porosity of ~58%. It is shown that the porous microstructure reduces the Young's modulus of the samples from 0.63 MPa (homogeneous) to 27 kPa (porous) and does not appreciably alter their magnetic properties.

DOI: 10.3103/S1062873823702015

INTRODUCTION

Magnetically active elastomers, a new class of smart materials with the properties controllable by a magnetic field, are being intensively studied due to the broad prospects for their application in such fields as biomedicine, sensors, and electronics [1–3].

One of the most common polymer bases for the synthesis of elastomer composites is polydimethylsiloxane (PDMS), which belongs to a group of polymeric organosilicon compounds also known as silicones. Structural features make them polymers with unique physical (elasticity, heat resistance, and dielectric strength) and chemical (inertness and hydrophobicity) characteristics. PDMS is also known for its intriguing rheological (flowing) properties. It is optically transparent and nontoxic, making it attractive for biomedical applications (scaffolds [4], implants [5], and lenses [6]). The functionalization of PDMS-based elastomers through manufacturing the composites with magnetic additives will allow the development of a promising field known as soft robotics, which is associated with the creation of miniature object manipulation systems controlled remotely by magnetic fields [7, 8].

Special attention in this area has been given to elastomers with porous structures [9–12]. This would allow us to considerably alter the mechanical properties of a material, since it reduces the density of the latter, expands the range of possible deformations, and makes the material more pliable to external factors. Porous elastomers based on PDMS in combination with conductive carbon nanotubes or graphene have already proven to be highly promising candidates for next-generation flexible electronics [13]. Porous PDMS with multi-walled carbon tubes has also demonstrated the ability to detect ultra-small strains and pressures over a wide operating range [14]. NdFeB micropowder fillers used in the production of permanent magnets are used most often in studies on magnetic elastomers. An alternative to NdFeB is magnetic oxides based on M-type hexaferrites with the general formula $MFe_{12}O_{19}$ ($M = Ba^{2+}$, Sr^{2+}, Pb^{2+}), which—in addition to their high saturation magnetization and coercivity—are more cost-efficient, chemically stable, corrosion resistant, and low-density [15, 16]. The aim of this work was to synthesize and explore PDMS and barium hexaferrite-based magnetic elastomers with different microstructures (homogeneous and porous), and to compare their magnetic and mechanical properties in order to establish the possibility of using them as actuators of magnetic field–driven valves.

EXPERIMENTAL

Our BaFO/PDMS magnetic elastomer samples were composites consisting of barium hexaferrite $BaFe_{12}O_{19}$ (BaFO) microparticles distributed in a PDMS polymer matrix (Fig. 1a). Magnetic particles were ordered in a magnetic field in one chosen direction (Fig. 1b).

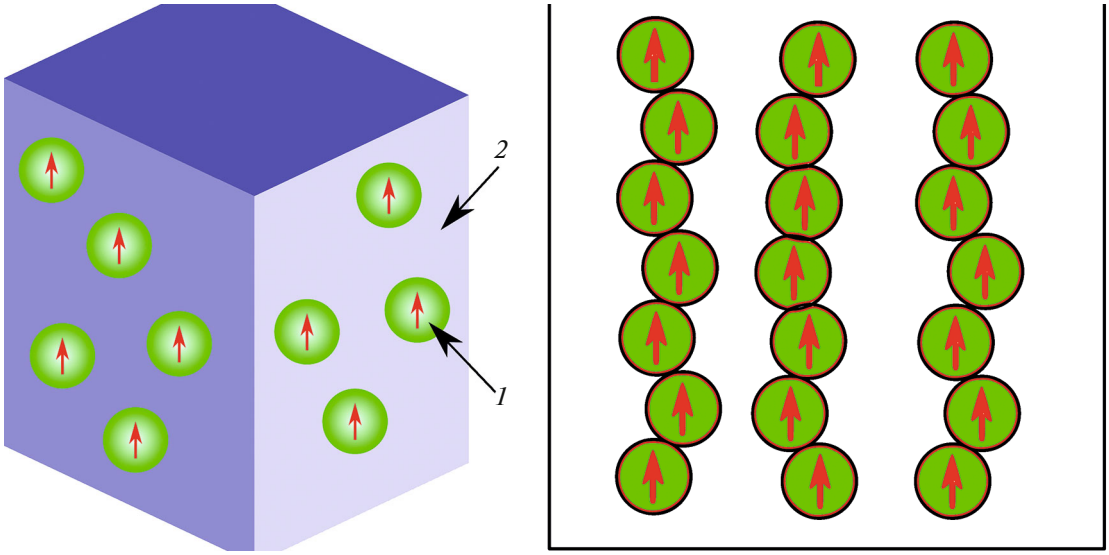

Fig. 1. (a) General model of the magnetic composite elastomer: barium hexaferrite microparticles (*1*) and polydimethylsiloxane matrix (*2*). (b) Schematic of magnetic particle ordering in the polymer matrix.

Samples of two types were obtained and examined. The first included a homogeneous BaFO/PDMS composite and pure PDMS samples. The second was samples of similar composition, but with a porous structure.

The elastomer composite samples were synthesized by curing a Rexant PK-68 two-component silicone compound added with magnetic microparticles using the polycondensation reaction. Polymerization of linear PDMS polymers into a crosslinked elastomer was done using a crosslinking reaction in which a platinum-based catalyst catalyzed the adding of Si–H bonds to vinyl groups with the formation of Si–CH_2–CH_2–Si bonds. To accomplish this, a mixture of low-molecular-weight dimethyloxane (base) and the catalyst was prepared in the required proportions (100 parts of the base to 5 parts of the catalyst). Two grams of this mixture was then poured into a Petri dish, and prepared barium hexaferrite magnetic microparticles were added. The concentration of BaFO microparticles was 16 wt % of the total composite mass. A powder of hard magnetic BaFO microparticles was obtained via the mechanical grinding of a commercial $BaFe_{12}O_{19}$ barium hexaferrite magnet in a ball mill for 30 min, followed by drying and sieving in a sieve with a mesh size of 40 μm. The final mixture consisting of the two-component compound with the magnetic particle additives was dried for 24 h at a temperature of 24°C until it was completely cured. A magnetic field of 0.1 T was applied perpendicular to the plane of the Petri dish throughout the curing of the elastomer samples.

Similar porous elastomer samples were synthesized by the leaching of fillers [17, 18]. The technique assumes the use of a filler soluble in a medium inert to the polymer matrix. The porosity and pore size of the sample are determined by the size and concentration of the filler. We used edible sugar granules 0.5–0.8 mm in size as a washable filler. The porous samples were obtained using a procedure similar to the synthesis of smooth samples, but with adding sugar granules to the PDMS polymer in a mass ratio of 1 : 1. After the final curing, the filler was washed out by soaking the samples in 100 mL of distilled water in an ultrasonic bath for at least 60 min while periodically squeezing the water from the sample until the complete dissolution and washing out of the sugar granules was achieved. When the procedure was complete, the samples were dried in an oven for 24 h at a temperature of 60°C. Four elastomer samples were obtained: pure PDMS, a BaFO/PDMS composite, porous PDMS, and a porous BaFO/PDMS composite. The microstructure of the samples and the geometry and sizes of pores were studied on a Cheetah YXLON X-ray control unit with a computed tomography function (Germany) that had a spatial resolution of at least 1 μm.

The magnetic properties of the samples were studied with a Lakeshore 7400 vibrating sample magnetometer. The temperature stability of the samples was determined via thermogravimetry using a NETZSCH TG 209 F3 Tarsus thermobalance. The Young's moduli of the samples were determined by measuring their elongation under static mechanical tension. The Young's modulus was determined from the elongation of each sample in the form of a rectangular plate under suspended loads of different masses. Each sample was suspended vertically from a tripod leg with a clamp. A plastic plate was placed between the samples and the clamp to ensure a more uniform distribution of the clamping stress. Loads with different nominal weights were attached to the lower end of the sample strip. Since inhomogeneous deformations arose at the samples' fastening points, stretching was measured not over an entire strip, but in the part of it located at a cer-

tain distance from the clamps. The uniform deformation determined in the experiment therefore did not depend on the inhomogeneous deformations at the place where the sample was fastened.

The Young's modulus was determined using the formula

$$E = \frac{F/S}{x/l}, \quad (1)$$

where F is the absolute value of the sample stretching force, S is the surface area over which force F is distributed, x is the absolute value of the change in the sample's length when deformed, and l is the length of the unstrained sample. The coefficient of proportionality between the stresses in the measured part of the sample strip caused by the applied forces and the relative elongation of this part of the strip (the Young's modulus) was determined according to least squares.

The porosity of the samples was determined from the difference between the masses of the porous sample in the dry and wet states, using the formula

$$n = \left(1 - \frac{\rho_V}{\rho_{dr}}\right) \times 100\%, \quad (2)$$

where

$$\rho_V = \frac{m_{dr}}{V_{dr}}, \quad (3)$$

$$\rho_{dr} = \frac{m_{dr}}{V}, \quad (4)$$

$$V = \frac{m_{dr} - m_{wet}}{\rho_{H_2O}}, \quad (5)$$

$$V_{dr} = \pi r^2 h, \quad (6)$$

where m_{dr} is the mass of the dry sample, m_{wet} is the mass of the water-wet sample, ρ_{H_2O} is the density of water, r is the radius of the sample, and h is the height of the sample.

RESULTS AND DISCUSSION

Figure 2 shows 3D X-ray computer tomography images of our homogeneous and porous BaFO/PDMS samples. Despite the identical masses of the initial components and the final samples, their thicknesses differ considerably because of the porous structure of one of the composite samples. The pore diameter was determined by the size of crystallites (their agglomerations) of the leachable filler in the PDMS polymer matrix. The microtomography images of the homogeneous and porous samples (Figs. 2a and 2b) clearly show the ordering of magnetic particles (light background) in the PDMS matrix, which was retained after PDMS polymerization and switching off the applied magnetic field. The measured Young's moduli and porosities of the samples are given in Table 1. The Young's modulus of the homogeneous samples is greater than that of the porous one by an order of magnitude (0.24–0.63 MPa for the smooth samples versus 24–27 kPa for the porous ones).

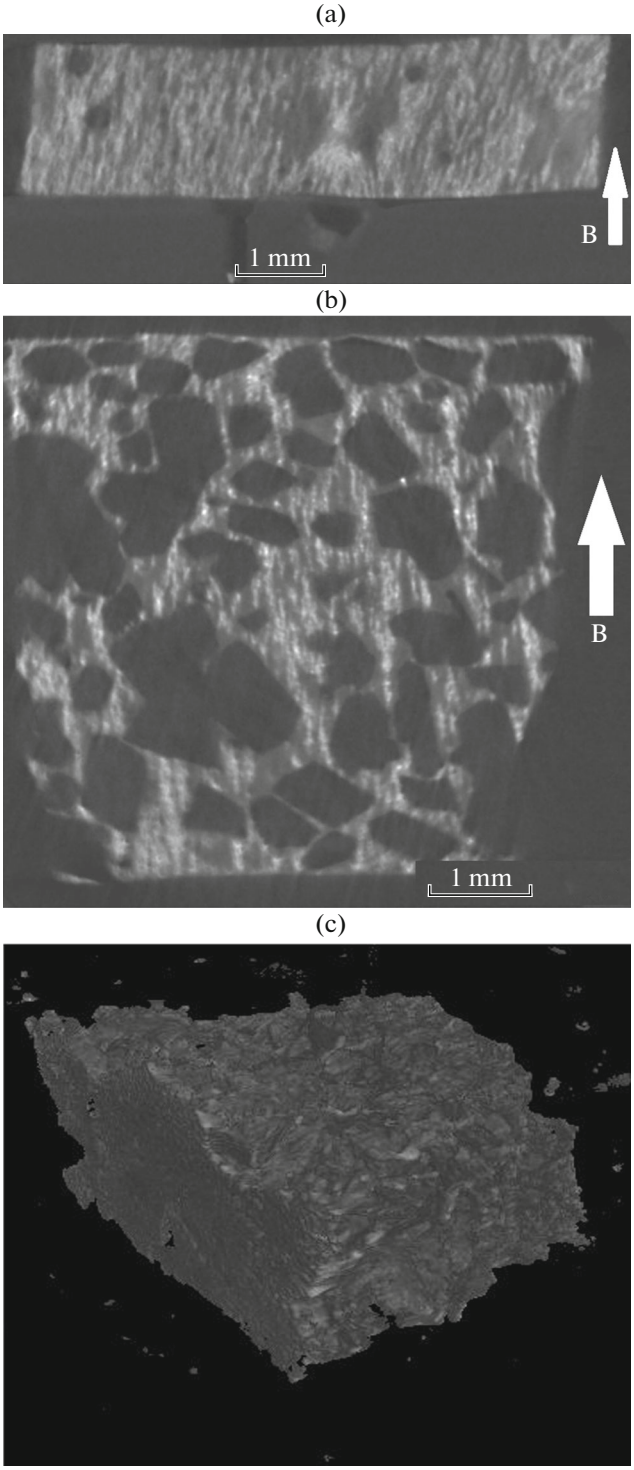

Fig. 2. 3D X-ray computer tomography cross-section micrographs of our (a) homogeneous and (b) porous BaFO/PDMS samples. (c) Microtomography image of the porous BaFO/PDMS sample.

We obtained the magnetic field dependences of magnetization (hysteresis loops) for the samples con-

Table 1. Porosities and Young's moduli of our PDMS and BaFO/PDMS composite samples

	Pure PDMS	BaFO/PDMS composite	Porous PDMS	Porous BaFO/PDMS composite
Young's modulus, MPa	0.24 ± 0.03	0.63 ± 0.10	0.024 ± 0.007	0.027 ± 0.005
Porosity, %	0	0	54	58

taining magnetic particles (Fig. 3a). For purposes of comparison, similar measurements were made for the powder of these particles without the polymer matrix (Fig. 3b). As can be seen from the plots, the porous structure of the polymer did not affect the magnetic properties of the samples, while the magnetic properties of the composite differed from those of the particles themselves. A comparison of the remnant magnetization of the samples and that of the powder ($M_r = 0.71M_s$ for the samples at $M_r = 0.44M_s$ for the particle

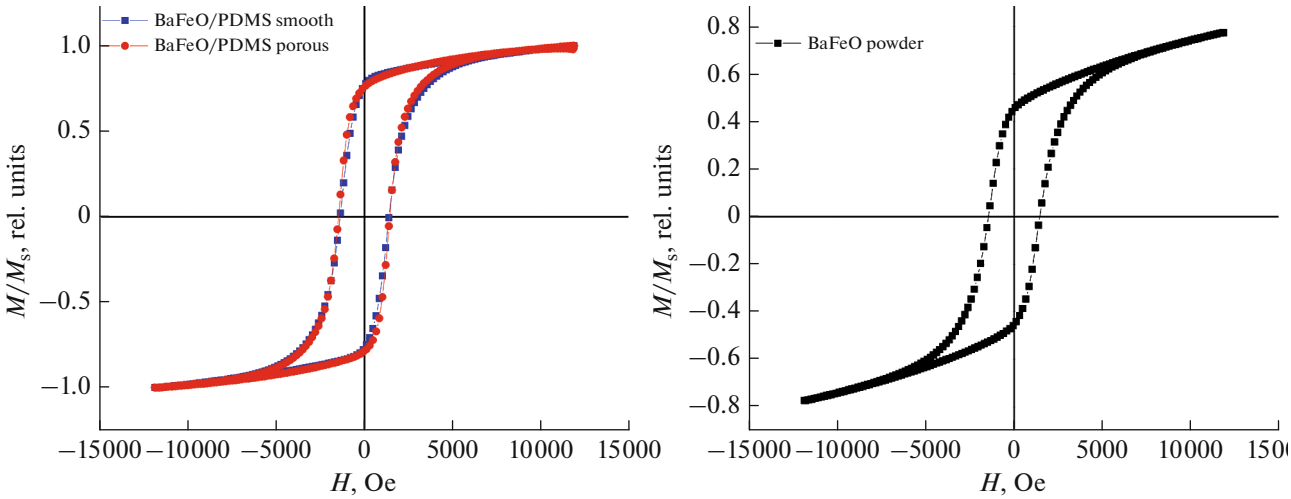

Fig. 3. Normalized magnetic field dependences of the magnetization (hysteresis loops) for (a) the homogeneous BaFO/PDMS composite (blue squares), porous BaFO/PDMS composite (red dots) with $M_s \approx 8.0$ erg/(G g), $M_r = 0.71M_s$, and $H_c = 1460$ Oe; and (b) for the barium hexaferrite powder with no polymer matrix: $M_s = 80$ erg/(G g), $M_r = 0.44M_s$, and $H_c = 1460$ Oe.

Fig. 4. Prototype demonstrating the operating principle of the magnetic field–driven valve: plastic valve base (*1*), porous BaFO/PDMS (*2*), porous BaFO/PDMS end (*3*) fixed to the base in (a) the closed state and (b) the open state when a nonuniform magnetic field is applied to the valve (the direction of the field is indicated by the arrow).

powder) shows that curing in a magnetic field determined the direction of easy magnetization (magnetic anisotropy) in the samples. The composites and the particle powder also had the same coercivity: H_c = 1460 Oe and $M_s \approx 8.0$ erg/(G g) for the composites and $M_s = 80$ erg/(G g) for the particles.

Our thermogravimetry measurements showed the obtained PDMS-based composites were destroyed at temperatures of ~740 K.

Comparative observations showed that the porous samples bent much more than the smooth ones in an identical magnetic field. Control with a magnetic field was therefore easier to achieve on the porous magnetic elastomer samples. The porous structure of the composite made it lighter, more pliable, and more elastic, so the porous samples were more suitable for use in magnetic field–driven devices. We designed a prototype to demonstrate the operating principle of a magnetic valve based on PDMS with barium hexaferrite microparticles (Fig. 4). The prototype was a plastic base with a hole for inserting the porous composite material. One side of the composite was connected to the edge of the base hole, while the other sides were in contact with but not connected to the base (Fig. 4a). When a nonunifrom magnetic field was applied to the prototype, the composite material bent and touched the base with its fixed side, thereby opening the valve (Fig. 4b). After switching off the magnetic field, the elastomer returned to its initial position due to its elasticity and closed the valve.

CONCLUSIONS

We studied the magnetic and mechanical properties of a homogeneous porous magnetic elastomer with a PDMS matrix and a barium hexaferrite microparticle filler. We found that due to its higher elasticity and pliability, a porous sample was more suited for use in a soft magnetic field-driven valve without deterioration of its magnetic properties than a sample with a homogeneous microstructure.

ACKNOWLEDGMENTS

The authors are grateful to A.S. Omelyanchik for his valuable advice and discussion of the results.

FUNDING

This work was supported by the Russian Science Foundation, project no. 21-72-30032 "Synthesis of Composites and Their Magnetic and Mechanical Properties." A.P. Pyatakov and A.S. Kaminskiy are grateful for the support of the BASIS Foundation for the Advancement of Theoretical Physics and Mathematics.

CONFLICT OF INTEREST

The authors declare that they have no conflicts of interest.

REFERENCES

1. Eduok, U., Faye, O., and Szpunar, J., *Prog. Org. Coat.*, 2017, vol. 111, p. 124.
2. Kolesnikova, V.G., Makarova, L.A., Omelyanchik, A.S., et al., *J. Magn. Magn. Mater.*, 2022, vol. 558, p. 169506.
3. Stepanov, G.V., Kramarenko, E.Yu., Perov, N.S., et al., *Vestn. Perm. Nats. Issled. Politekh. Univ., Mekh.*, 2013, no. 4, p. 106.
4. Li, J., Liu, X., Crook, J.M., et al., *Colloids Surf., B*, 2017, vol. 159, p. 386.
5. Dunn, K.W., Hall, P.N., and Khoo, C.T.K., *Br. J. Plast. Surg.*, 1992, vol. 45, no. 4, p. 315.
6. Chen, J.S., Liu, T.Y., Tsou, H.M., et al., *J. Polymer Res.*, 2017, vol. 24, no. 5, p. 69.
7. Kim, Y., Parada, G.A., Liu, S., and Zhao, X., *Sci. Rob.*, 2019, vol. 4, no. 33, p. eaax7329.
8. Xu, T., Zhang, J., Salehizadeh, M., et al., *Sci. Rob.*, 2019, vol. 4, no. 29, p. eaav4494.
9. Zhao, X., Li, L., Li, B., et al., *J. Mater. Chem. A*, 2014, vol. 2, no. 43, p. 18281.
10. Choi, S.J., Kwon, T.H., Im, H., et al., *ACS Appl. Mater. Interfaces*, 2011, vol. 3, no. 12, p. 4552.
11. Li, J., Liu, X., Crook, J.M., et al., *Colloids Surf., B*, 2017, vol. 159, p. 386.
12. Cha, K.J. and Kim, D.S., *Biomed. Microdevices*, 2011, vol. 13, no. 5, p. 877.
13. Duan, S., Yang, K., Wang, Z., et al., *ACS Appl. Mater. Interfaces*, 2016, vol. 8, no. 3, p. 2187.
14. Iglio, R., Mariani, S., Robbiano, V., et al., *ACS Appl. Mater. Interfaces*, 2018, vol. 10, no. 16, p. 13877.
15. Pullar, R.C., *Prog. Mater. Sci.*, 2012, vol. 57, no. 7, p. 1191.
16. Vinnik, D.A., Zherebtsov, D.A., Mashkovtseva, L.S., et al., *Cryst. Growth Des.*, 2014, vol. 14, no. 11, p. 5834.
17. Ribeiro, C., Costa, C.M., Correia, D.M., et al., *Nat. Protoc.*, 2018, vol. 13, no. 4, p. 681.
18. González-Rivera, J., Iglio, R., Barillaro, G., et al., *Polymers*, 2018, vol. 10, no. 6, p. 616.

Translated by E. Bondareva